Indonesian Journal of Electrical Engineering and Computer Science
Vol. 24, No. 1, October 2021, pp. 295~307
ISSN: 2502-4752, DOI: 10.11591/ijeecs.v24.i1.pp295-307

Ultra low bitrate retinal image compression using integer lifting scheme and subband encoder

Yassine Habchi[1], Ameur Fethi Aimer[2], Mohammed Beladgham[3], Riyadh Bouddou[4]
[1]Laboratory of TIT (UTMB-Bechar), Department of Technology, Institute of Science and Technology, University Center Salhi Ahmed, Naama, Algeria
[2]Diagnosis group, LDEE Laboratory (USTO-Oran), Department of Electrical Engineering, University of Saida, Saida, Algeria
[3]Laboratory of TIT (UTMB-Bechar), Department of Electrical Engineering, Tahri Mohammed University, Bechar, Algeria
[4]Departement of Electrotechnics, IRECOM Laboratory, University of Sidi Bel-Abbes, Algeria

Article Info

Article history:

Received Jun 1, 2021
Revised Aug 12, 2021
Accepted Aug 23, 2021

Keywords:

Color retinal image
Blood vessels
Subband encoder
Integer lifting scheme
Cohen daubechies-feaveau wavelet

ABSTRACT

Recently, ophthalmic clinics have seen many complaints related to retinal diseases. The degree of clarity of the blood vessels (BV) in the eye can be an important indicator of some diseases affecting the retina such as diabetic retinopathy. To diagnose it, we need to intervene more than a medical team, especially in some difficult cases, through the exchange of medical images obtained by photography. This method has contributed significantly to the production of large data that can quickly saturate transmission, storage systems and increase processing time, so the need to compress images efficiently without modifying the content before transmission represents a major challenge. This paper provides an effective method for compressing color retinal images (CRI), which relies on the use of an integer lifting scheme (ILS) based on cohen daubechies-feaveau wavelet (CDFW9/7) and the set partitioning in hierarchical trees (SPIHT) to encode large coefficients. The obtained results demonstrate that the suggested method reduce algorithmic complexity, improve the retinal image quality and achieves high objective parameters values for ultra-low bitrate compared to the conventional methods.

Corresponding Author:

Yassine Habchi
Laboratory of TIT (UTMB-Bechar), Technology Department
Institute of Science and Technology
University Center Salhi Ahmed, Naama, Algeria
Email: habchi.jjl@gmail.com

1. INTRODUCTION

The clarity of ocular images during endoscopic examination helps ophthalmologists diagnosis of diseases such as diabetic retinopathy, which is one of the main causes of diabetic blindness and high blood pressure. The retina is the lining of the eye and its function lies in the sense of light coming to the eye, consisting of large blood vessels (BV) (veins) and BV accurate (arteries) easy to damage, and that high blood sugar for a long time can damage these vessels. These changes in the lining of BV increase their permeability [1], [2]. At first, some of these vessels develop and weaken, and these vessels get clogged and do not allow enough blood to pass through them. New BV grow in the place of clogged vessels. These new vessels are weak and easily ruptured, so blood leaks into the glass liquid in the eye. This blood prevents light from reaching the retina. The patient may notice floating spots or a dark area covering the whole eye. This

blood sometimes goes away alone but may need surgery. Identifying the structure of BV is therefore important in the diagnosis of eye diseases like micro aneurysm and hemorrhage [3].

In some cases where retinal diseases are difficult to diagnose, the use of highly sophisticated technologies such as telemedicine, which facilitates the sharing of diagnosis by more than one specialized medical team, involves the transfer, distribution, collection, exchange and the retrieval and processing of medical information automatically in the form of images and through the media, which may be very exposed to types of noise. These adversely affect the quality of the clarity of images and thus the results of medical diagnosis [4]. The increasing volume and change of medical data for patients, which undoubtedly exceed the limits of human memory, contributes significantly to the saturation of transport and storage systems and the consequent decline in hospital efficiency in the health service; for this, many advanced image compression algorithms have been used [5]. To handle this type of images on medical ophthalmology, several works based on wavelet transform (WT) in retinal image processing are proposed, we can cite for example in [6], the authors propose an efficient technology based on discrete wavelet transformation (DWT) in the process of removing the optical disc (OD) of the green original image, to avoid misclassification between exudates region and OD. Kokare [7], used wavelets to analyze and detect various secretions in retinal images. In [8], the authors proposed an algorithm based on pre-processing, vessel extraction, and post-processing to facilitate the extraction of large and thin affected BV in retinal images using a 2D gabor filter followed by linear Hough transform. In [9], the authors used the wavelet-based RIQA algorithm to partition a retinal image into subbands of detail. Kausu *et al.* [10], proposed a method for glaucoma identification based on dual-tree complex wavelet. In [11], wavelet is used to extracts textural features of the retinal images. In [12], propose to use WT to detect the optic disc and BV. In [13], the authors deal with the problem of image quality degradation with compression ratio in observer-based diagnostic accuracy, where they used wavelet compression to produce opposite trends in detection.

This method presents an advantage over JPEG in terms of robustness. However, the main problem is that significant labelling errors will have occurred above compression ratios (CR). In [14], the authors addressed the problem of retinal image compression, where they prouve that the G channel in the color retinal image compression has more information than other channels. In [15], the authors focous on upon region of interest (ROI) of retinal images where they present an efficient retinal image compression method based on modified Huffman method. This method is mainly based on the pre-processing with an adaptive median filter, segmentation using improved adaptive fuzzy c-means clustering, compression using integer multi wavelet transform and set partitioning in hierarchical trees algorithms respectively. An algorithm for identifying vessels on the optic disc is described in [16]. The five module method (FMM) has been used to take compressed retinal images as the input. The vessel is findded using watershed lines and canny detectors. Different features are extracted and labeled as normal abnormal using support vector machine (SVM) classifier. In [17], representation dictionary (RD), enhancement dictionary (ED) and sparse coding technology have been used to enhance the target vessel retinal images. Also, in [18] a comparative study is introduced to compress digital retinal images using JPEG and wavelet for different level of compression. In [19], an efficient coder based on discrete cosine transform (DCT) has been used by authors to compress retinal image. In [20], a quantitative analysis of the effects of JPEG image compression of retinal fundus camera images on vessel segmentation and on morphometric vascular measurements are reported. Vascular assessment and measurement platform for images of the retina (VAMPIRE) has been used for measurement of digital retinal images for vessel extraction (DRIVE), automated retinal image analyzer (ARIA), high-resolution fundus (HRF).

However, in the early 1990s Sweldens [21] and Daubechies [22], implemented efficiently the discrete wavelet with new scheme named as The ILS, where it characterized with perfect reconstruction granted by the structure of the scheme itself. In this paper, we provide an effective approach to solve the following problems: First, we focus on the degree and accuracy of the CRI content in low bitrates areas; second, we reduce the sheer volume of medical data without affecting the content [23]. The proposed algorithm is than based mainly on the use of ILS based CDF wavelet [24] and SPIHT encoder [25]. The main contribution of this work is summarized as follows; First, the ILS based on CDFW9/7 is used to extract image features and reduce algorithmic complexity. Hence, it can get values of decorrelated coefficients. Second, the SPIHT is chosen to encode produced coefficients wavelets to define lists according to the coefficients efficiency. Third, the strong relationships between the red, green and blue components in color medical image (CMI) are reduced, for this the three components RGB are transformed to luminance and chrominance (YCbCr) coordinates. Finally, the green channel of the CRI is chosen, this is due to the low contrast of blue channel, so few information have appeared and the noise in red channel which causes the saturation. The experimental results demonstrate that the proposed method outperforms existing methods in terms of peak signal to noise ratio (PSNR) and mean structural similarity (MSSIM). Currently, in the literature there is no similar work where it is based on the compression of CRI based on the structure of ILS and SPIHT encoder.

The remainder of this paper is arranged as follows: the basic concepts of the retinal image coding are described in section 2. Simulation result and discussion are provided in section 3 and finally the conclusions are given in the section 4.

2. RESEARCH METHOD

At the end of the 1970s and the beginning of the 1980s, wavelet has established an excellent reputation with a suggestion of the geophysicist Jean Morlet as a powerful alternative scan to the conventional transform (e.g. fourier transform and discrete cosine transform) for the local properties of complex signals. The central drawback of the fourier transform is that Joseph Fourier could not display temporal information; it considered that each signal could be represented only on frequencies. For discrete cosine transform known with blocking artifacts at low bitrates and with its discontinuities when more compression is required at block boundaries. A wasteful process of detailed information in the image can occur when reducing blocking defects with any filter smoothing. In the late 1980s, Ingrid daubechies constructed a family of wavelet bases to extract essential information from a signal. In 1984, Alex Grossman and Jean Morlet proved the property of energy conservation. In 1986, Yves Meyer developed its major works related to the improvement of the mathematical theory of wavelets. After a few years, Stephane Mallat contributed in a fundamental way to the development of wavelet theory with applications like medical imaging. He collaborated with Yves Meyer to develop multiresolution analysis and discovered a relationship between wavelets and filter banks. The WT is a basic function of multi-resolution variation, it serves as a mathematical zoom, which can be used for analysis and synthesis of multidimensional signals through its pyramidal decomposition via a family of translated and dilated wavelets into scaling and wavelet function [26]-[29].

The scaling function is defined with the following expression:

$$\phi_{j,n}(t) = \left\{ \frac{1}{\sqrt{2^j}} \phi\left(\frac{t-n}{2^j} \right) \right\}_{(j,n)\in\mathbb{Z}2} \tag{1}$$

and the orthonormal wavelet basis can be defined as:

$$\psi_{j,n}(t) = \left\{ \frac{1}{\sqrt{2^j}} \psi\left(\frac{t-2^j n}{2^j} \right) \right\}_{(j,n)\in\mathbb{Z}2} \tag{2}$$

In the case of image, we have fourth subband an approximation function $\varphi(t)$ and three mother wavelets functions $\psi^H(x)$, $\psi^V(x)$, and $\psi^D(x)$ with $x = (x_1, x_2) \in R^2$ are dilated by 2^j and translated by $2^j n$ with $n = (n_1, n_2) \in \mathbb{Z}^2$. This yield an orthonormal basis of the space $L^2(\mathbb{R}^2)$:

$$\psi^k_{j,n}(x) = \left\{ \frac{1}{2^j} \psi^k \left(\frac{x-2^j n}{2^j} \right) \right\}_{j\in Z, n\in Z^2, 1\le k\le 3} \tag{3}$$

In practice, such transforms are directly chosen to be used on specific disciplines (e.g., telecommunication, medical imaging, and multidimensional signal processing), where the extraction of the target information needs high accuracy. However to increase the wavelets properties, the classical wavelets are replaced by another types proposed by Sweldens (1998) [30], named as the ILS where has been applied on image horizontally and then vertically, respectively.

This scheme enhances the speed of wavelet decomposition, has no quantization errors and does not require auxiliary memory. Hence, it has become popular with more efficient performance. In our study, this structure is used to enhance the efficiency of the suggested work where the property of perfect reconstruction is guaranteed.

Such structures are desired for the representation of retinal images on several levels of resolution. From a formal point of view, a ILS is a bank which consists of the split/merge, predict and update. These steps are discussed as:

A. The forward ILS

– Split: The input signal $(X[n])$ is split into odd indexed points $(X_{odd}[n]=X[2n+1])$ and even indexed samples $(X_{even}[n]=X[2n])$.

– Prediction (P): It is used to obtain detail coefficients $(d[n])$ as the error prediction of (X_{odd}) from (X_{even}) by using the predict operator (P). $(d[n]=X_{odd}[n]-P(X_{even}[n]))$

– Update (U): In this step, the (X_{even}) and $(d[n])$ are combined by applying the update operator (U) to the $(d[n])$ in order to obtain scaling coefficients $(c[n])$. $(c[n]=X_{even}[n]+U(d[n]))$

B. The inverse ILS

– Undo update: $(X_{even}[n]=c[n]-U(d[n]))$

– Undo predict: $(X_{odd}[n]=d[n]+P(X_{even}[n]))$

– Merge: $(X[n]=X_{even}[n]+X_{odd}[n])$

For the CDFW9/7, two prediction operators and two update operators are obtained using ILS, where ILS coefficient of CDFW9/7 are defined as: $\alpha(1.586134342060)$, $\gamma(0.882911075531)$ denote the prediction coefficients, $\beta(0.052980118573)$, $\delta(0.443506852044)$ denote the update coefficients and $\xi(1.149604398860)$ represents the scaling factor [31] as shown by the following expressions a detailed example is show in the Figure 1.

$$d_i = x_{2i+1} + \alpha\left(x_{2i} + x_{2i+2}\right) \tag{4}$$

$$s_i = x_{2i} + \beta\left(d_{i-1} + d_i\right) \tag{5}$$

$$d'_i = k_e\left[d_i + \gamma\left(s_i + s_{i+1}\right)\right] \tag{6}$$

$$s'_i = k_0\left[s_i + \delta\left(d'_{i-1} + d'_i\right)\right] \tag{7}$$

where $i=0,1,2,...,(M-1)/2$, M represents the input data

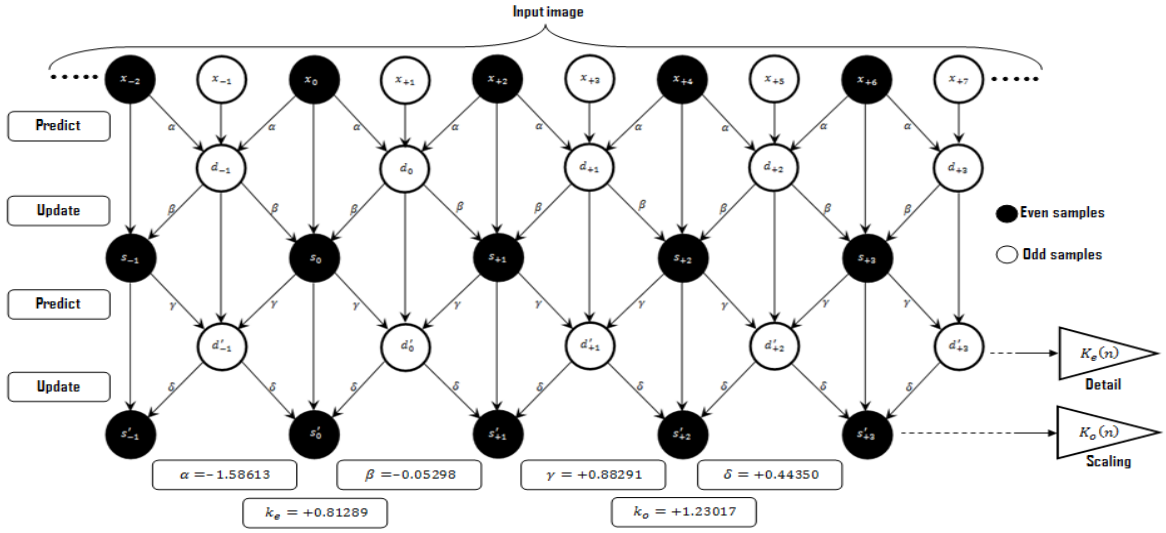

Figure 1. The forward CDFW9/7 using ILS

At each iteration, the coefficients are oversampled by a factor of two and coded by SPIHT. The SPIHT is as the embedded zerotrees of wavelet transforms (EZW) [32]; it is based on performing a recursive partitioning of the sorting coefficients into the spatial orientation tree in order to specify a relationship between parents and children/grandchildren at higher and lower levels respectively and its position in the tree as it shown in Figure 2. The same principle of coding the significant coefficients in EZW is the same in SPIHT which consists of three lists: list of significant coefficients (LSC), list of insignificant coefficients (LIC) and list of insignificant sets (LIS). The reasons of selecting SPIHT, because it is an efficient image compression algorithm that exploits the inherent similarities across the subbands in a wavelet decomposition of CRI.

The algorithm proceeds in the following manner: The LSC is initially empty, while the LIC contains the coarser scale coefficients of the LL sub-band and its all descendants are put in the LIS of each tree. Firstly, the significant test is done against the threshold for all elements in the LIC and giving the 0 or 1 in the output bitstream. All significant coefficients are displaced to the LSC. Also, the significant test is done for the entire set in the LIS.

If a set is significant, it is partitioned into offspring where the initial partition is segmented recursively by the following rule: The node is divided to the four child coefficients and the LIC or LSC received all descendants when the set of descendants of appropriate node is significant. The SPIHT does a refinement pass in the end of the processing of all elements of the list LIC and LIS (sorting pass). In the end of sorting pass and refinement pass, the all coefficients are coded by an effective entropy coding. The block diagram of our proposed algorithm is illustrated in Figure 3.

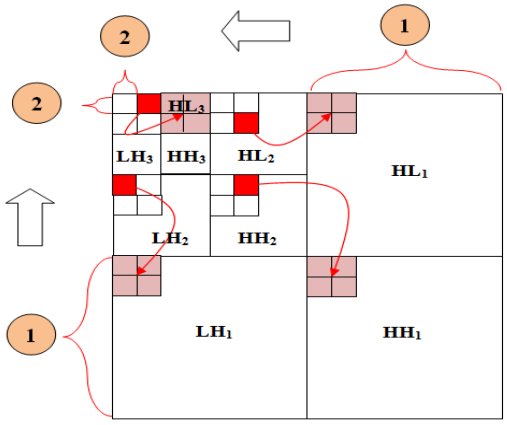

Figure 2. 2D wavelet decomposition, three level. 1: Finer scale wavelet coefficients; 2: coarser scale wavelet coefficients

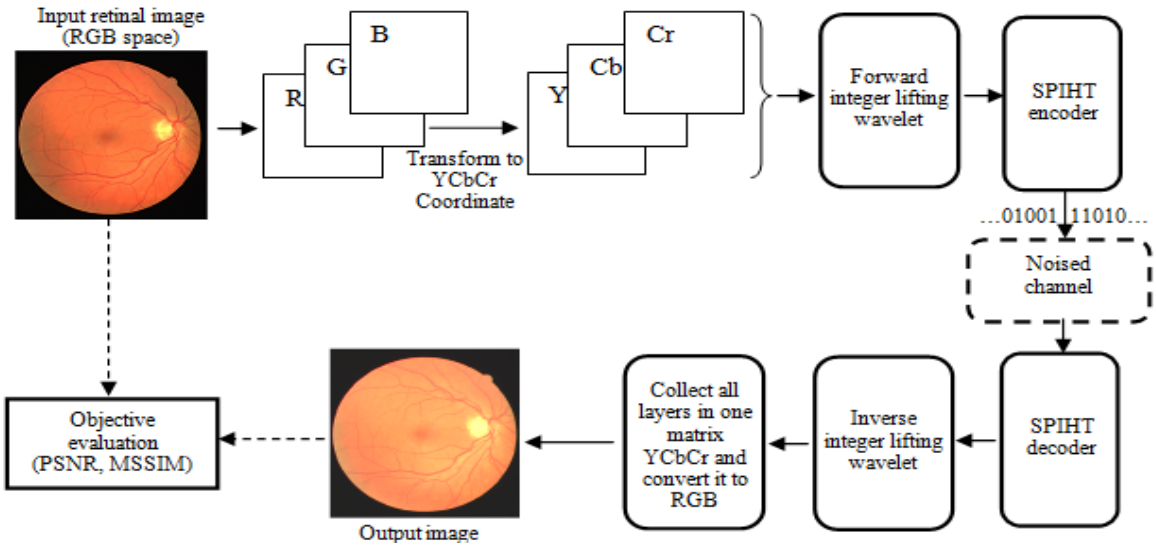

Figure 3. Block diagram showing the principal retinal BV image compression

3. RESULTS AND DISCUSSION

The proposed SPIHT wavelet coding results are presented in this section. To ensure the effectiveness of the suggested algorithm, numerical experiments have been done on a set of the color pathological medical images of size 256x256, coded at 24 bits per pixel (bpp) with 8bpp being allocated to red, green and blue colors which include retinal, melanoma, intestinal metaplasia and Mri (Magnetic resonance imaging) image [33], using MATLAB R2010a on an Intel(R) Core (TM): 3-5005U CPU@2.00GHz 2.00GHz. The set of retinal images used for evaluation are obtained from retina identification database (RIDB), which is a retinal image database comprised of 100 Fundus Images with 1504 × 1000 resolution compressed in JPEG format has been captured using TOPCON-TRC Fundoscope. The main objective of this test is to obtain a high visual quality image for low bitrate. For this, the bitrate is varied from 0.015625bpp to 1bpp and objective parameters are calculated to the each corresponding proposed algorithms:

– 1st ALGO: CDFW9/7 coupled to SPIHT encoder applied to color image,
– 2nd ALGO: CDFW9/7 coupled to SPIHT encoder applied to green image,
– 3rd ALGO: ILS-CDFW9/7 coupled to SPIHT encoder applied to green image.

The reasons of selecting CDFW9/7, because they are from a family of biorthogonal wavelets that are not the same as the other orthogonal Daubechies wavelets.

The peak signal to noise ratio (PSNR) and mean structural similarity (MSSIM) are two important objective evaluation metrics where they were relied upon in the evaluation of RGB medical image quality. It is true that the PSNR is a good objective metric for the visual quality measurement of the image, but this is not in all cases due to several reasons, including that is needed the original and resultant image to determine the difference between them. Also, it does not give enough information about subjective evaluations of the image. Therefore is not a very suitable parameter for the image visual quality assessment. Hence, in our assessment of the obtained results, we relied on other metric named by the structural similarity scale (SSIM) distinguished by providing enough information about all image features accurately [34].

The three channels of CRI are shown in Figure 4. Before performing the algorithm to each color and in order to reduce the strong relationship between the red, green and blue components in CMI, the three components RGB are transformed to luminance and chrominance (YCbCr) coordinates and treated them as three greyscale images separately.

Where:

– Luminance (Y): received brightness of the light.
– Chrominance (Cb, Cr): describe the perceived color tone of a light.

The YCbCr values in the YUV coordinates are related to the RGB values in the RGB coordinates by:

$$\begin{pmatrix} Y \\ Cb \\ Cr \end{pmatrix} = \begin{pmatrix} 0.299 & 0.587 & 0.114 \\ -0.16875 & -0.33126 & 0.500 \\ 0.5 & -0.41869 & -0.08131 \end{pmatrix} \begin{pmatrix} R \\ G \\ B \end{pmatrix} \quad (8)$$

The transformation from YCbCr to RGB is given by:

$$\begin{pmatrix} R \\ G \\ B \end{pmatrix} = \begin{pmatrix} 1 & 0 & 1.402 \\ 1 & -0.34413 & -0.71414 \\ 1 & 1.772 & 0 \end{pmatrix} \begin{pmatrix} Y \\ Cb \\ Cr \end{pmatrix} \quad (9)$$

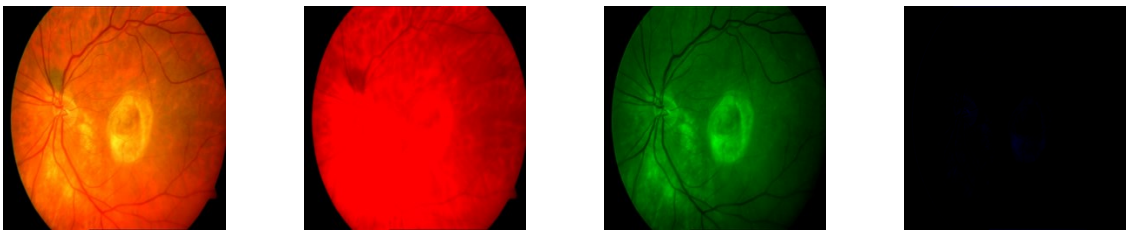

(a) (b) (c) (d)

Figure 4. RGB retinal image with its component (a) original image, (b) red component, (c) green component and (d) blue component

The fundus image is based on the automated analysis of the green channel. This is due to the low contrast of blue channel; so, few information have appeared in Figure 4(d) and the noise in red channel in Figure 4(b) which causes the saturation. For this reason, in our proposed work, we have chosen the green channel of the CRI where we can see clearly that the image shown in Figure 4(c) is well-contrasted and clear then blue and red channel image consecutively. In our algorithm, each component of the input image is decomposed into a five-level using wavelet CDFW9/7. An example of the green (Cb) component decomposition is shown in Figure 5. The highest amplitudes of ILS coefficients compared to the wavelets have been represented as histograms in Figure 6.

The proposed (3rd ALGO) algorithm has been compared against (1st ALGO and 2nd ALGO). In addition, Figure 7 shows the comparison in terms of PSNR(dB) values at several bitrates (from 0.25bpp to 1bpp) between (1st ALGO and 2nd ALGO) algorithms. By comparing the different values of PSNR(dB), we show clearly the effectiveness of the 2nd ALGO of compressed retinal image quality. Other comparatives visual results applied to other CRI using 3rd ALG at 1bpp are shown in Figures 8 and 9, where the important results have been shown for Retinal-E. For a fair evaluation of the performance, the results of the proposed algorithm (3rd ALGO), tested on other set medical images of the same size: 'Melanoma', 'Intestinal metaplasia' and 'Mri', are reported in Figures 10-13.

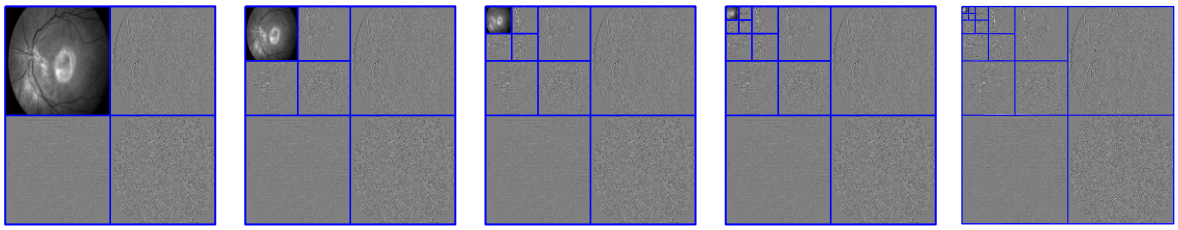

Figure 5. The green (Cb) component decomposition of retinal image: subbands of five-level decomposition: (a) one level, (b) two level, (c) three level, (d) four level and (e) five level

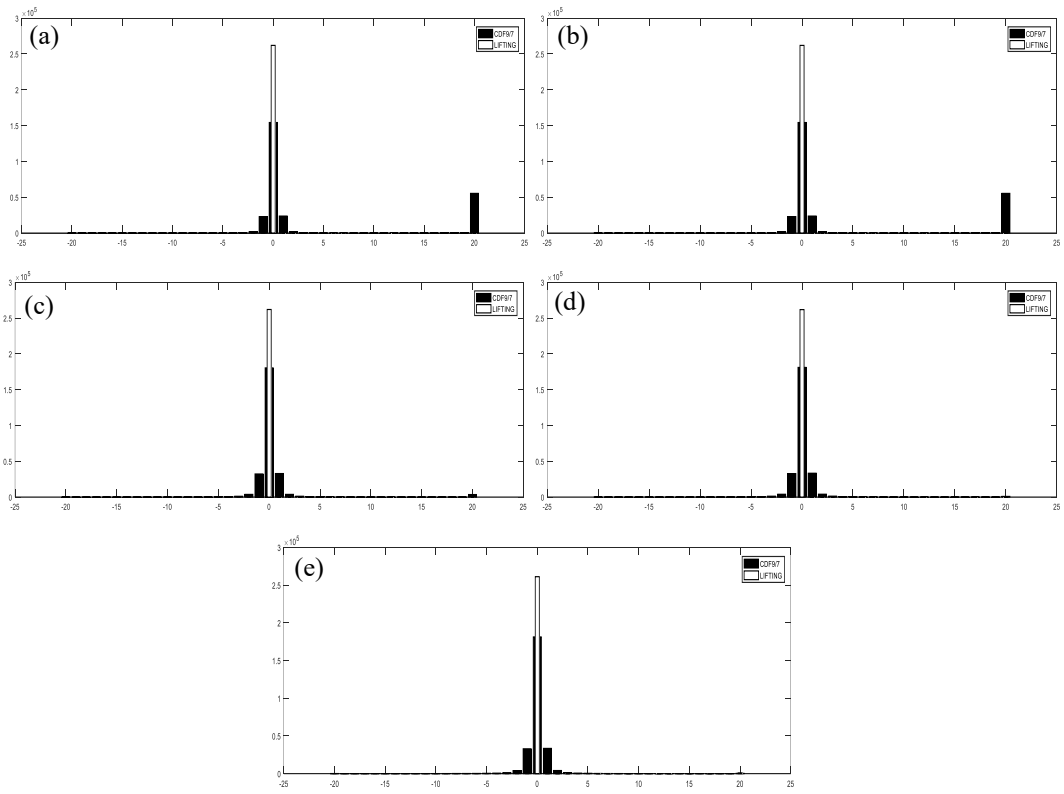

Figure 6. RGB (YCbCr) retinal image histogram coefficients: (a) 1st level decomposition, (b) 2nd level decomposition, (c) 3rd level decomposition, (d) 4th level decomposition and (e) 5th level decomposition

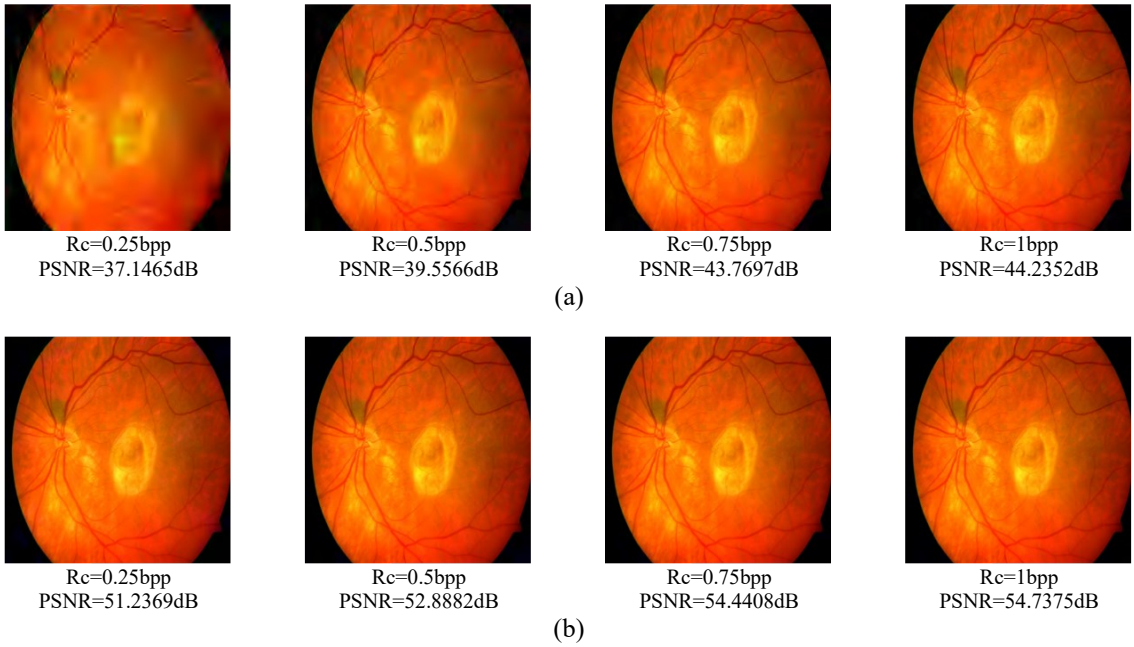

Figure 7. Recovered visual results of CRI using (a) 1st ALGO and (b) 2nd ALGO

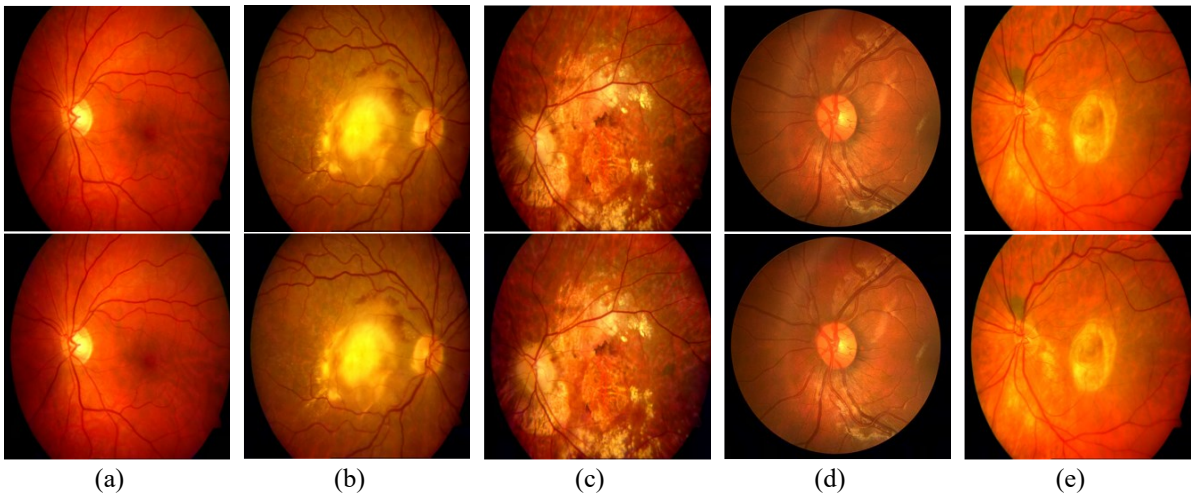

Figure 8. Comparative visual results between other original (top row) and recovered (bottom row) CRI using 3rd ALG at 1bpp: (a) retinal-A, (b) retinal-B, (c) retinal-C, (d) retinal-D and (e) retinal-E

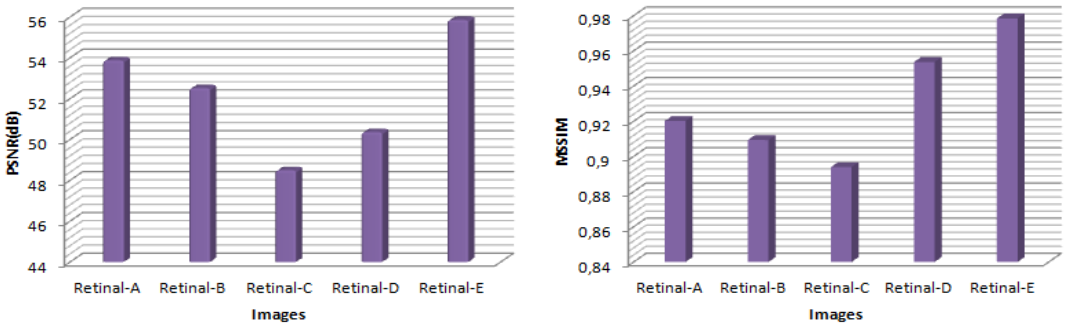

Figure 9. Results of PSNR(dB) and MSSIM for different CRI using 3rd ALG at 1bpp

- Melanoma is a type of cancer that occurs in cells containing pigment.
- Intestinal metaplasia is the transformation of epithelium into a type of epithelium resembling that found in the intestine.
- Magnetic resonance imaging (Mri) is used in radiology to form images.

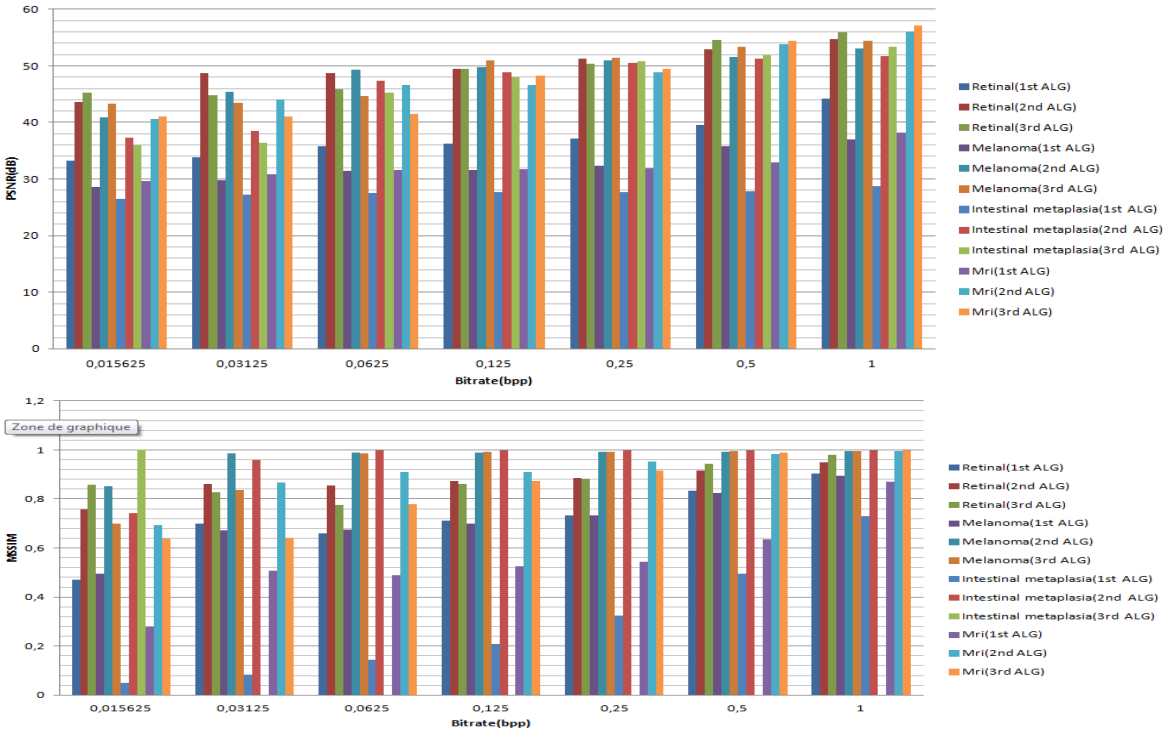

Figure 10. The comparison results between 1st ALGO, 2nd ALGO and 3rd ALGO for different medical color images in term of PSNR(dB) and MSSIM

Figure 11. Results of PSNR(dB) and MSSIM gain for different medical color images. G1 represent the gain between the 1st and 2nd ALGO; G2 represent the gain between the 2nd and 3rd ALGO

Through Figure 10, it is clear that the proposed method (3rd ALGO) of compressing medical images is very efficient compared to the 1st ALGO and 2nd ALGO for all bit-rates and this is through highest values of PSNR(dB) and MSSIM. The PSNR(dB) gain exceeds 1dB at very low bit-rates for all tested medical images. The improvement achieved through the results is very clear compared to the 1st ALGO and 2nd ALGO. For example, the gain reaches 1,7419dB for 'Retinal', 2,3722dB for 'Melanoma', 1,5856 for 'Intestinal metaplasia' and 1,6512 for 'Mri'. The gain PSNR alternate between 10 to 20 dB between the 1st and 2nd ALGO and is alternate between 0 to 2dB in the range [0.015625–1] bpp for all tested medical images.

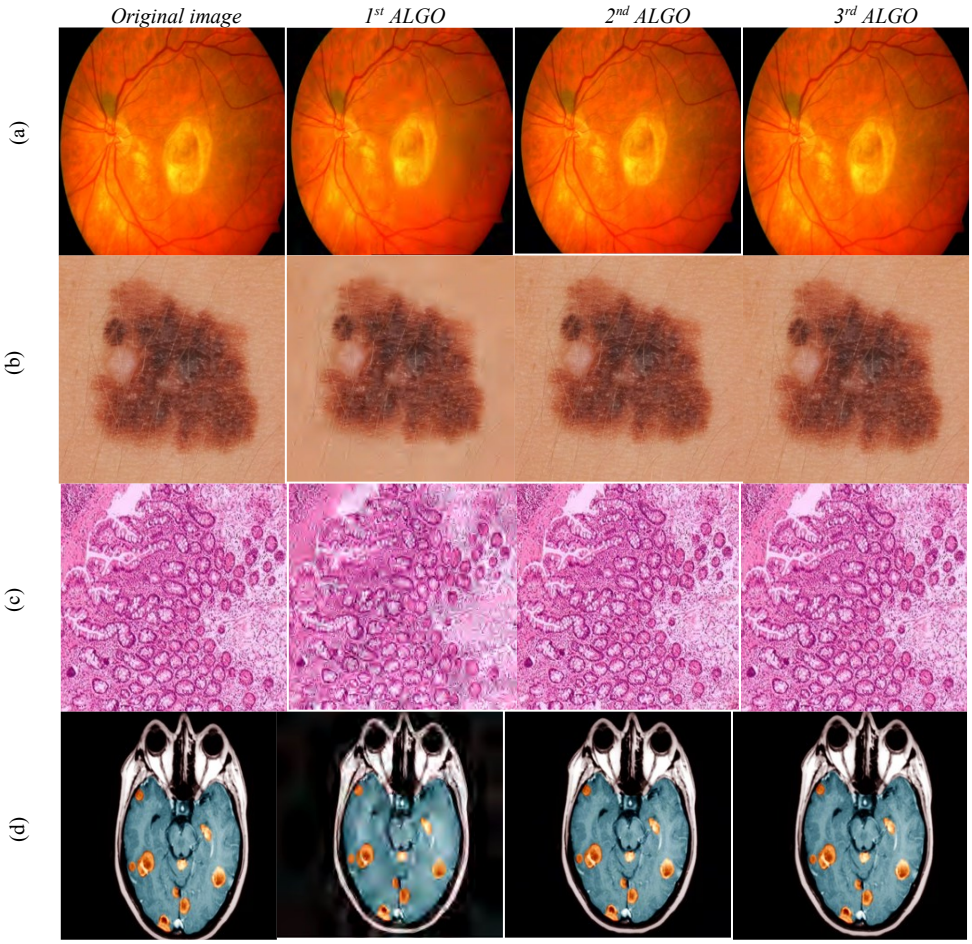

Figure 12. The visual assessment results at 1bpp: (a) retinal, (b) melanoma, (c) intestinal metaplasia, and (d) Mri

Figures 12 and 13 shows the recover 'Retinal', 'Melanoma', 'Intestinal metaplasia' and 'Mri' images of size 256×256 for first, second and third algorithms at 1bpp. From this figures, it can be observed that the visual quality of the compressed images with 3rd ALGO is very better than that of 1st ALGO and 2nd ALGO where this difference becomes more apparent and confirmed precisely by presented results in Figure 11 through the values of Gain1 (G1) and Gain2 (G2).

The improvement, variety and efficiency of gain depending on the content of the tested images and the bit-rate values. In overall, the results demonstrate clearly that the CMI is better exploited by the proposed algorithm. The results between the three algorithms for different CMI in term of computational time (in seconds) are presented in Table 1. The computational time obtained by the third algorithm (in bold values) is better than the first and the second algorithm for CRI.

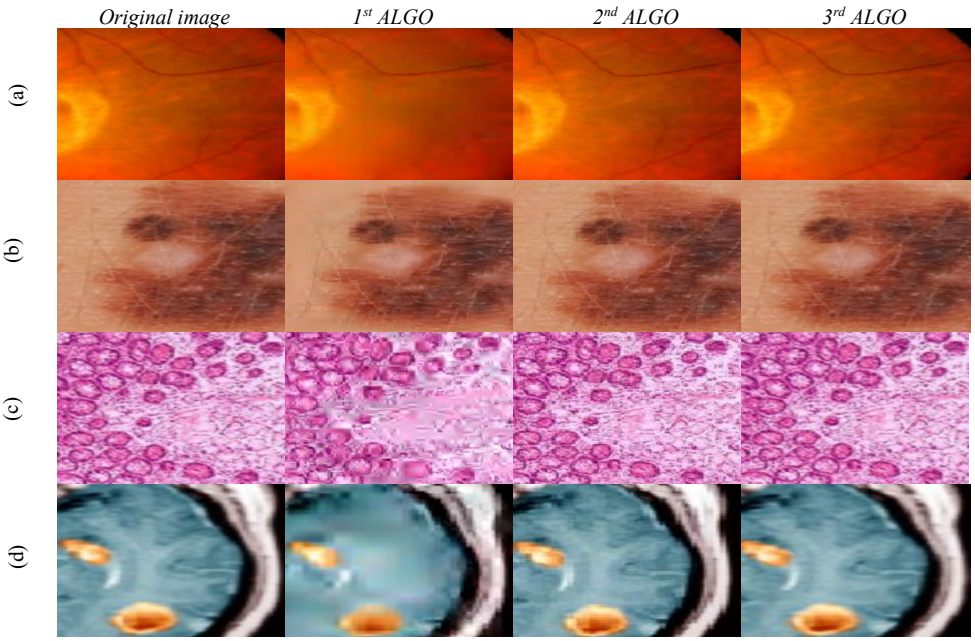

Figure 13. Region of interest (ROI) at 1bpp: (a) retinal, (b) melanoma, (c) intestinal metaplasia and (d) Mri

Table 1. The comparison results between 1st ALGO, 2nd ALGO and 3rd ALGO for CRI in term of computational time (in seconds)

Bitrate (bbp)	1st ALGO	2nd ALGO	3rd ALGO	Gain1	Gain2
0.015625	2.023086	2.600515	**2.080294**	0.0572	**-0.5202**
0.03125	2.255999	2.322372	**2.123703**	**-0.1323**	**-0.1987**
0.0625	2.211291	2.248560	**2.169353**	**-0.0419**	**-0.0792**
0.125	2.066577	2.185377	2.213179	0.1466	0.0278
0.25	2.168468	2.386188	**2.208262**	0.0398	**-0.1779**
0.5	2.342272	2.509429	**2.338652**	**-0.0036**	**-0.1708**
1	3.284376	3.314453	**3.098860**	**-0.1855**	**-0.2156**

The best obtained results are indicated with **bold** values in terms of computational time. Gain1 represent the gain between the 3rd and 1st ALGO; Gain2 represent the gain between the 3rd and 2nd ALGO.

4. CONCLUSION

In this paper, we studied BV discovery during the compression process through the use of an effective WT based on the use of ILS and SPIHT encoder. The correlation included in the retinal medical image is well exploited with a new construction of wavelets, called the ILS while the SPIHT encoder is used to encode significant coefficients. However, in order to improve results and retinal image quality, it was suggested that the compression process should be limited to the green channel. The proposed algorithm has shown better results and high visual quality for CRI at any given bit-rate for all test images.

REFERENCES

[1] A. Ali, W. W. Zaki, and A. Hussain, "Retinal blood vessel segmentation from retinal image using b-cosfire and adaptive thresholding," *Indonesian Journal of Electrical Engineering and Computer Science (IJEECS)*, vol. 13, no. 3, pp. 1199-1207, 2019, doi: 10.11591/ijeecs.v13.i3.pp1199-1207.

[2] D. Devaraj and P. K. SC, "Development of a hybrid framework to charac-terize red lesions for early detection of diabetic retinopathy," *Indonesian Journal of Electrical Engineering and Computer Science(IJEECS)*, vol. 13, no. 3, pp. 962-973, 2019, doi: 10.11591/ijeecs.v13.i3.pp962-973.

[3] R. Phellan, T. Lindner, M. Helle, A. X. Falcao, and N. D. Forkert, "Au-tomatic temporal segmentation of vessels of the brain using 4d asl mraimages," *IEEE transactions on biomedical engineering*, vol. 65, no. 7, pp. 1486-1494, 2017, doi: 10.1109/TBME.2017.2759730.

[4] T. A. Soomro, T. M. Khan, M. A. Khan, J. Gao, M. Paul, and L. Zheng,"Impact of ica-based image enhancement technique on retinal blood vesselssegmentation," *IEEE Access*, vol. 6, pp. 3524-3538, 2018, doi: 10.1109/ACCESS.2018.2794463.

[5] K. Marlapalli, R. S. Bandlamudi, R. Busi, V. Pranav, and B. Madhavrao,"A review on image compression techniques," *inCommunication Softwareand Networks,* Springer, 2021, pp. 271-279, 10.1007/978-981-15-5397-4_29.

[6] S. Bharkad, "Automatic segmentation of exudates in retinal images," in *2018 International Conference on Wireless Communications, Signal Pro-cessing and Networking (WiSPNET)*, IEEE, 2018, pp. 1-5, doi: 10.1109/WiSPNET.2018.8538644.
[7] P. Kokare, "Wavelet based automatic exudates detection in diabeticretinopathy," in *2017 International Conference on Wireless Communica-tions, Signal Processing and Networking (WiSPNET)*, IEEE, 2017, pp. 1022-1025, doi: 10.1109/WiSPNET.2017.8299917.
[8] P. Nazari and H. Pourghassem, "An automated vessel segmentation al-gorithm in retinal images using 2d gabor wavelet," in *2013 8th IranianConference on Machine Vision and Image Processing (MVIP),* IEEE, 2013, pp. 145-149, doi: 10.1109/IranianMVIP.2013.6779967.
[9] L. Abdel-Hamid, A. El-Rafei, S. El-Ramly, G. Michelson, and J. Hornegger, "Retinal image quality assessment based on image clarity and content," *Journal of biomedical optics*, vol. 21, no. 9, p. 096007, 2016, doi: 10.1117/1.JBO.21.9.096007.
[10] T. Kausu, V. P. Gopi, K. A. Wahid, W. Doma, and S. I. Niwas, "Combi-nation of clinical and multiresolution features for glaucoma detection andits classification using fundus images," *Biocybernetics and Biomedical Engineering*, vol. 38, no. 2, pp. 329-341, 2018, doi: 10.1016/j.bbe.2018.02.003.
[11] A. Khademi and S. Krishnan, "Shift-invariant discrete wavelet transformanalysis for retinal image classification," *Medical & biological engineering& computing*, vol. 45, no. 12, pp. 1211-1222, 2007, doi: 10.1007/s11517-007-0273-z.
[12] L. C. Rodrigues and M. Marengoni, "Segmentation of optic disc and bloodvessels in retinal images using wavelets, mathematical morphology andhessian-based multi-scale filtering," *Biomedical signal processing and con-trol*, vol. 36, pp. 39-49, 2017, doi: 10.5220/0005317006170622.
[13] P. H¨ansgen, P. Undrill, and M. Cree, "The application of wavelets to retinalimage compression and its effect on automatic microaneurysm analysis," *Computer methods and programs in biomedicine*, vol. 56, no. 1, pp. 1-10, 1998, doi: 10.1016/S0169-2607(98)00006-6.
[14] A. W. Setiawan and A. Faisal, "A study on jpeg compression in color retinalimage using bt. 601 and bt. 709 standards: Image quality assessment vs.file size," in *2020 International Seminar on Application for Technology ofInformation and Communication (iSemantic),* IEEE, 2020, pp. 436-441, doi: 10.1109/iSemantic50169.2020.9234245.
[15] N. Salih, A. Abid, and C. Eswaran, "Efficient retinal image compressionbased on modified huffman algorithm," *International Journal of Engineering Research and Technology*, vol. 12, no. 7, pp. 942-948, 2019.
[16] S. Akshay and P. Apoorva, "Segmentation and classification of fmm com-pressed retinal images using watershed and canny segmentation and supportvector machine," in *2017 International Conference on Communication andSignal Processing (ICCSP),* IEEE, 2017, pp. 1035-1039, doi: 10.1109/ICCSP.2017.8286531.
[17] B. Gu, B. Chen, and L. Luo, "Retinal vessel enhancement via sparse codingand dictionary learning," in *2017 Fifteenth IAPR International Conferenceon Machine Vision Applications (MVA)*, IEEE, 2017, pp. 270-273, doi: 10.23919/MVA.2017.7986853.
[18] R. H. Eikelboom *et al.,* "Methods and limits of digital imagecompression of retinal images for telemedicine," *Investigative Ophthalmology & Visual Science*, vol. 41, no. 7, pp. 1916-1924, 2000.
[19] S. Krivenko, V. Lukin, O. Krylova, and V. Shutko, "Visually lossless com-pression of retina images," in *2018 IEEE 38th International Conference onElectronics and Nanotechnology (ELNANO)*, IEEE, 2018, pp. 255-260, doi: 10.1109/ELNANO.2018.8477459.
[20] M. R. K. Mookiah, S. Hogg, T. MacGillivray, and E. Trucco, "On the quan-titative effects of compression of retinal fundus images on morphometricvascular measurements in vampire," *Computer Methods and Programs inBiomedicine*, vol. 202, p. 105969, 2021, doi: 10.1016/j.cmpb.2021.105969.
[21] W. Sweldens, "The lifting scheme: A custom-design construction ofbiorthogonal wavelets," Applied and Computational Harmonic Analysis, vol. 3, no. 2, pp. 186-200, 1996, doi: 10.1006/ACHA.1996.0015.
[22] I. Daubechies and W. Sweldens, "Factoring wavelet transforms into liftingsteps," *Journal Of Fourier Analysis And Applications*, vol. 4, no. 3, pp. 247-269, 1998, doi: 10.1007/BF02476026.
[23] T. Samakande, T. Shongwe, A. S. de Beer, and H. C. Ferreira, "The effectof coupling circuits on impulsive noise in power line communication," in *2018 IEEE International Symposium on Power Line Communications andits Applications (ISPLC)*, IEEE, 2018, pp. 1-5, doi: 10.1109/ISPLC.2018.8360232.
[24] K. B. Rekha and K. A. Ravi, "Design of high speed lifting based dwt using9/7 wavelet transform for image compression," in *2017 International Con-ference on Recent Advances in Electronics and Communication Technology (ICRAECT)*, IEEE, 2017, pp. 132-137, doi: 0.1109/ICRAECT.2017.38.
[25] A. Said and W. A. Pearlman, "A new, fast, and efficient image codec basedon set partitioning in hierarchical trees," *IEEE Transactions on circuits andsystems for video technology*, vol. 6, no. 3, pp. 243-250, 1996, doi: 10.1109/76.499834.
[26] R. Karthikeyan and G. Hegde, "High performance vlsi architecture for 3-ddwt (discrete wavelet transform)," in *2018 2nd International Conferenceon Inventive Systems and Control (ICISC),* IEEE, 2018, pp. 892-897, doi: 10.1109/ICISC.2018.8398929.
[27] I. Daubechies, "Ten lectures on wavelets," *SIAM*, 1992, doi: 10.1137/1.9781611970104.
[28] N. Khanna, V. Kumar, and S. Kaushik, "Wavelet packet approximation," *Integral Transforms and Special Functions*, vol. 27, no. 9, pp. 698-714,2016, doi: 10.1080/10652469.2016.1189912.
[29] N. Khanna, S. Kaushik, and A. Jarrah, "Wavelet packets: Uniform approx-imation and numerical integration," *International Journal of Wavelets, Multiresolution and Information Processing*, vol. 18, no. 02, p. 2050004, 2020, doi: 10.1142/S0219691320500046.

[30] I. Daubechies and W. Sweldens, "Factoring wavelet transforms into liftingsteps," in *Wavelets in the Geosciences*, Springer, 2000, pp. 131-157, doi: https: 10.1007/BF02476026.
[31] S. H. Dabhole and S. T. Jadhav, "An efficient codec of 2d adaptive direc-tional lifting based on cdf9/7 with improved spiht algorithm for lossy tolossless image coding," in *2015 2nd International Conference on Electronicsand Communication Systems (ICECS)*, IEEE, 2015, pp. 84-91, doi: 10.1109/ECS.2015.7125031.
[32] J. M. Shapiro, "An embedded hierarchical image coder using zerotrees ofwavelet coefficients," in *Proceedings DCC93: Data Compression Conference,* IEEE, 1993, pp. 214-223, doi: 10.1109/DCC.1993.253128.
[33] Available online: www.eyecharity.com/aria online/. Accessed: 2020-02-13.
[34] H. R. Sheikh and A. C. Bovik, "Image information and visual quality," *IEEE Transactions on image processing*, vol. 15, no. 2, pp. 430-444, 2006, doi: 10.1109/TIP.2005.859378.

BIOGRAPHIES OF AUTHORS

Yassine Habchi, got his Engineering Degree in Electronics in 2010 at the University of saida Dr MOULAY Tahar. Magister was the second degree in signal and digital communication at Tahri Mohammed University of Bechar in 2013. Since May 2017, he graduated PhD Es Sciences at the University of Bechar. He did his research at the University Center Salhi Ahmed Naama and Laboratory of TIT (UTMB-Bechar). His research interests are Medical Imaging, Signal, Image and Video processing, Wavelets Analysis, Data Compression, Deep Learning, Renewable Energy. E-mail: habchi.jjl@gmail.com

Ameur Fethi Aimer was born on August 23, 1983 in Saida, Algeria. He received his Engineering degree in electrical engineering from the University of Saida in 2006, his Magister degree and his Doctorate of Sciences degree in industrial control of electric drives and diagnosis from the University of Sciences and Technology of Oran, Algeria in 2010 and 2018 respectively. He is currently a Senior Lecturer at the University of Saida. His research interests include Electric Drives, Signal Processing as well as Electric Machines Faults Diagnosis. Dr. AIMER is a member of the Diagnosis Group (Laboratory of Electrical Drives Development - USTO-Oran. Algeria). E-mail: fethi.aimer@yahoo.fr

Mohammed Beladgham, was born in Tlemcen, Algeria. He received the electric engineering diploma from university of Tlemcen, Algeria, and then a Magister in signals and systems from university of Tlemcen, Algeria and the Ph.D. degree in Electronics from the University of Tlemcen (Algeria), in 2012. His research interests are Image processing, Medical image compression, wavelets transform and optimal encoder. E-mail: beladgham.tlm@gmail.com

Riyadh Bouddou was born in Mecheria, Algeria, in 1993. He received the Master's degree in Electrotechnical Engineering in 2018 from Djillali Liabes University of Sidi-Bel-Abbes, Algeria. He is currently a PhD candidate at Faculty of Electrical Engineering, Djillali Liabes University, a member in the research laboratory "IRECOM", a substitute professor at University Center of Naama and an IEEE student member. Fields of interest: Power System Analysis, Economic Dispatch, Optimal Power Flow, Renewable Energy, Electricity Markets and Metaheuristics. E-mail : riyadh.bouddou@univ-sba.dz